

**Purdue University**  
**Purdue e-Pubs**

---

International Refrigeration and Air Conditioning  
Conference

School of Mechanical Engineering

---

2004

# Experimental and Numerical Steady-State Analysis of a Top-Mount Refrigerator

Joaquim Manoel Goncalves

*Federal Center of Technological Education of Santa Catarina*

Claudio Melo

*Federal University of Santa Catarina*

Follow this and additional works at: <http://docs.lib.purdue.edu/iracc>

---

Goncalves, Joaquim Manoel and Melo, Claudio, "Experimental and Numerical Steady-State Analysis of a Top-Mount Refrigerator" (2004). *International Refrigeration and Air Conditioning Conference*. Paper 700.  
<http://docs.lib.purdue.edu/iracc/700>

This document has been made available through Purdue e-Pubs, a service of the Purdue University Libraries. Please contact [epubs@purdue.edu](mailto:epubs@purdue.edu) for additional information.

Complete proceedings may be acquired in print and on CD-ROM directly from the Ray W. Herrick Laboratories at <https://engineering.purdue.edu/Herrick/Events/orderlit.html>

## EXPERIMENTAL AND NUMERICAL STEADY-STATE ANALYSIS OF A TOP-MOUNT REFRIGERATOR

J. M. GONÇALVES<sup>1</sup>, C. MELO<sup>2</sup>

<sup>1</sup> Federal Center of Technological Education of Santa Catarina  
608, José Lino Kretzer St., Praia Comprida  
88103-310, São José, SC, Brazil  
+55 48 247 36 46, joaquim@sj.cefetsc.edu.br

<sup>2</sup> Federal University of Santa Catarina  
Department of Mechanical Engineering  
88040-900, Florianópolis, SC, Brazil  
+55 48 234 56 91, melo@nrva.ufsc.br

### ABSTRACT

The goal of this work is to study the steady-state behavior of a top-mount refrigerator by measuring and modeling the performance characteristics of each one of its components. Measurements of the relevant variables were taken at several positions along the refrigeration loop, generating performance data not only for the whole unit but also for each one of the components. The experiments were planned and performed following a statistically based methodology and considering 13 independent variables that led to over 160 data runs. The models were based on the mass, energy and momentum conservation principles and also on empirical data. The complete set of equations was implemented into and solved by the EES/REFPROP software. The model predictions for the refrigeration capacity and power consumption when compared with experimental data were within a  $\pm 10\%$  deviation band. The model was also used to simulate the effect of the system parameters on the refrigerator performance in an attempt to minimize the energy consumption for a given internal air temperature.

### 1. INTRODUCTION

Refrigeration systems consisting of a hermetic reciprocating compressor, a wire and tube condenser, a capillary tube-suction line heat exchanger and a finned-coil evaporator, such as household refrigerators and freezers, are widely used. Such systems, on the whole, consume a large amount of energy since hundreds of millions are currently in use and millions are coming onto the market every year. A knowledge of the operational characteristics of a refrigeration system is vital for any energy conservation study, not only for predicting the system performance, but for optimizing the combination of system components during the design process and also to provide insights into control strategies that may improve the system performance.

Many mathematical models have been proposed in the past for modeling refrigeration systems. In one of the earliest studies, Davis and Scott (1976) developed a mathematical model to predict the steady-state component behavior over a range of operating conditions. The overall model consisted of individual component models that combined basic principles with a number of empirical parameters. Yasuda et al. (1983) developed a simulation model for a vapor compression system, based on the energy conservation law, applied to the compressor, condenser and evaporator. Chi and Didion (1982) developed a simulation model for a heat pump, using a lumped modeling approach for each one of the components.

The methodology presented herein conjugates experimental and theoretical information into a computational model to represent the steady-state behavior of a refrigeration system. The experimental work consisted of controlling and measuring the system and component operating conditions in order to gather key information for the development and validation of the model. In order to do this the refrigeration system was properly and carefully instrumented to minimize any impact on its performance. The mass, energy and momentum conservation laws were used to establish

the governing equations that describe the system behavior. Each component was modeled using a lumped approach, based on physical principles and employing parametric constants fitted to the experimental data by the least square method. The main empirical parameters were the heat transfer and the friction factor coefficients. Such a model was able to predict the experimental test results with a reasonable level of agreement and was also able to simulate the system behavior for a given internal air temperature. It should be mentioned that this kind of analysis is crucial for the system design but almost impossible to perform using laboratory resources.

## 2. EXPERIMENTAL STUDY

The tests were performed with a 430-liter top-mount refrigerator, assembled with a hermetic reciprocating compressor, a wire and tube condenser, and a finned-coil forced flow evaporator. The system employed HFC-134a as the working fluid (130g) and synthetic oil as the lubricant (250 ml). The air temperatures in the freezer and in the fresh food compartments were controlled by a thermostat and a by a thermostatic damper, respectively.

The refrigerator was instrumented and installed inside an environmental chamber with controlled air temperature and humidity. Type T thermocouple probes immersed in the refrigerant flow passage and absolute pressure transducers were installed at seven points along the refrigeration loop, as shown in Figure 1. A Coriolis mass flow meter was installed in the discharge line. The outside air temperature was measured by 5 thermocouples placed around the refrigerator. The freezer and the fresh food compartment air temperatures were measured by 3 and 6 thermocouples placed inside the compartments, respectively. Tests were performed before and after the instrumentation set-up to check for any effect on system performance.

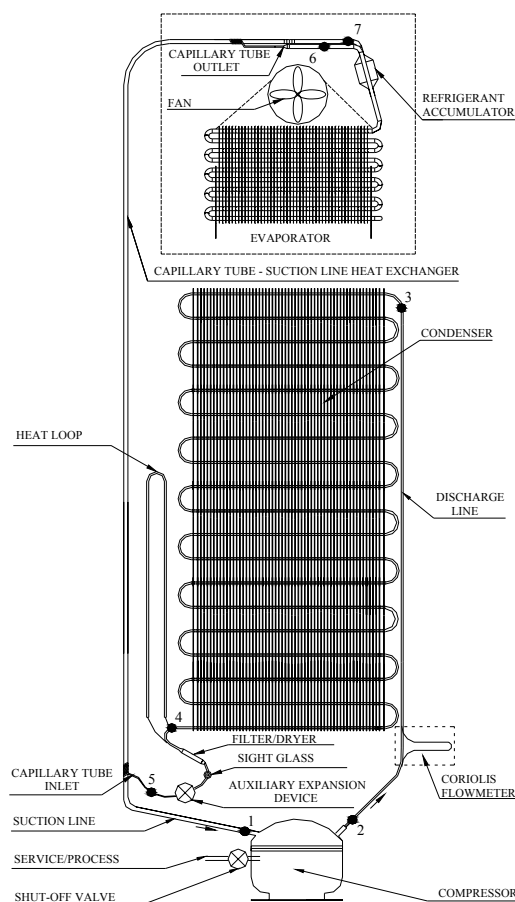


Figure 1: Instrumented refrigeration system

A small reduction in the system cooling capacity (less than 3%) was then detected. After this stage some adjustments were introduced into the system to allow the attainment of desired information.

A needle metering valve was installed as an auxiliary expansion device ahead of the capillary tube. The original compressor was replaced by a similar one but with variable speed. The wall heat loop was closed and the no-frost heaters turned off. The damper had its thermostatic mechanism removed and its aperture was kept constant. The compressor and fan power consumption and speed were controlled and measured independently. The three phase power consumption and speed of the variable speed compressor was measured with a power meter. The fan speed was measured with an electronic circuit using infrared light across its blades as the primary signal. In total 13 variables were experimentally studied, 7 were geometric characteristics of the system and the other 6 were operational variables. The geometric characteristics were varied in a combined way to generate 8 different system configurations (see Table 1). Each of these configuration tests were performed controlling the following 6 operational variables: ambient temperature, compressor speed, refrigerant charge, auxiliary expansion device opening, fan speed and internal heating. A total of 168 tests were performed, with around 20 tests for each system geometrical configuration. Independent experimental setups, not using the refrigerator itself, were used to measure the capillary tube inner diameter, the component internal volumes and the cabinet overall thermal conductance.

Figures 2 and 3 show an overview of the experimental measurements. The relationship between compressor power consumption and internal air temperature is illustrated in Figure 2, where a clear tendency towards lower consumption at higher internal air temperatures is shown. It should be pointed out that the higher air temperature values are mainly associated with lower refrigerant charge, compressor speed and expansion device opening. The range of tested conditions is showed in a P-h diagram in Figure 3.

Table 1: System geometric configurations

System #	Capillary tube				Condenser		Evaporator
	Length	Diameter	Inlet length	Diameter	Number of wires	Number of tubes	Number of fins
	[m]	[mm]	[m]	[mm]	[wires]	[tubes]	[fins]
1	3.0	0.64	0.2	4.8	55	19	47
2	4.0	0.60	0.4	5.6	45	19	58
3	4.0	0.75	1.6	5.6	75	19	29
4	3.0	0.75	0.2	5.6	65	19	35
5	3.0	0.56	0.2	4.8	90	25	35
6	3.0	0.56	0.8	6.2	60	13	47
7	4.0	0.64	0.4	4.8	30	25	29
8	4.0	0.75	1.6	4.8	60	25	58

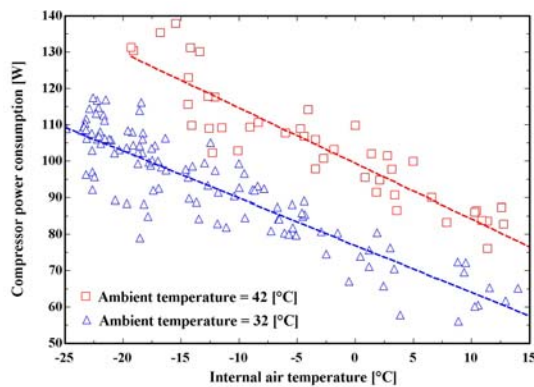


Figure 2 – Compressor power vs. internal air temperature

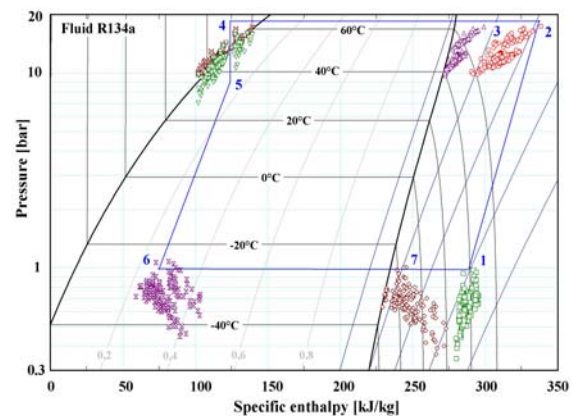


Figure 3 - Experimental data points

### 3. COMPONENTS MODELING

For modeling purposes the system was divided into 5 components: compressor, condenser, capillary tube, evaporator and suction line. As mentioned before the component models were based on the mass, energy and momentum conservation principles and also on empirical data. The basic principles yielded two equations for each component that were used to calculate the specific enthalpy and pressure at the interconnection points. The conservation of mass law applied as a mass inventory to the entire system supplied an additional equation for the mass flow rate. The energy conservation principle applied to the refrigerated cabinet supplied a final equation for the internal air temperature. The resulting set of non-linear equations was therefore composed of 12 equations and 12 unknowns.

#### 3.1 Compressor

The compressor mass flow rate equation was based on the volumetric efficiency (Gosney, 1984). In the compressor energy balance equation the power consumption was expressed in terms of an isentropic efficiency and the compressor heat released rate by an overall thermal conductance applied to the compressor shell and related to the temperature difference between the discharge line and the ambient air. The volumetric efficiency, isentropic coefficient and the overall thermal conductance of the shell were all fitted to the experimental data.

$$m = \frac{PD \cdot N}{v_1} \cdot \eta_V \quad (1)$$

$$m \cdot (h_2 - h_1) = W_{comp} - Q_{comp} = m \cdot (h_{2,s} - h_1) / \eta_s - (UA)_{comp} \cdot (T_2 - T_{amb}) \quad (2)$$

### 3.2 Condenser

The condenser heat transfer rate was modeled assuming a uniform air temperature distribution and using the  $\varepsilon$ -NTU concept (Kays and London, 1984). The condenser was divided into three regions depending on the refrigerant state: superheated, saturated or sub-cooled. Equation 4 has a more simplified format because the refrigerant temperature was also assumed to be uniform in this region.

$$Q_{sup} = m \cdot (h_2 - h_{vap}) = m \cdot c_P \cdot (T_2 - T_{amb}) \cdot (1 - e^{-(UA)_{sup}/m \cdot c_P}) \quad (3)$$

$$Q_{sat} = m \cdot (h_{vap} - h_{liq}) = U_{sat} \cdot A_{sat} \cdot (T_{cond} - T_{amb}) \quad (4)$$

$$Q_{sub} = m \cdot (h_{liq} - h_5) = m \cdot c_P \cdot (T_{cond} - T_{amb}) \cdot (1 - e^{-(UA)_{sub}/m \cdot c_P}) \quad (5)$$

For each region, the overall thermal conductance was obtained from the internal and external thermal resistance values, as shown in equation 6. The external thermal resistance was evaluated taking into account the finned area overall efficiency. The heat transfer coefficients were fitted to the experimental data. The internal heat transfer coefficient was adjusted for each region while the external was maintained constant for all regions. This approach is known as a three zone variable conductance model (Kempiak and Crawford, 1991). A decision algorithm was applied sequentially to equations 3 to 5 in order to identify the region under analysis.

$$(UA)^{-1} = R = R_{int} + R_{ext} = (htc_{int} \cdot A_{int})^{-1} + (\eta \cdot htc_{ext} \cdot A_{ext})^{-1} \quad (6)$$

The condenser pressure drop was modeled by the so-called Darcy-Weisbach equation, using the refrigerant properties at the component inlet. The friction factor was fitted to the experimental data.

$$\Delta P_{cond} = f \cdot \frac{L_{cond}}{D_{cond}} \cdot \frac{\rho V^2}{2} \quad (7)$$

### 3.3 Capillary Tube

The mass flow rate through the capillary tube was evaluated by a non-dimensional, Buckingham-Pi Theorem format equation, using a set of dimensionless parameters proposed by ASHRAE(2002). The equation coefficients were fitted to the experimental data provided by Zangari (1998) for sub-cooled inlet conditions and to the ones obtained in this work for saturated inlet conditions. When either the subcooling or quality approached zero the mass flow rate was determined by a linear interpolation between the values given by both equations.

The heat transfer in the capillary tube-suction line heat exchanger was determined using the heat exchanger concept of temperature effectiveness (Shah, 1996). The effectiveness was fitted to the experimental database of Zangari (1998), assuming a linear equation format dependent on the refrigerant mass flow rate, suction line inner diameter and heat exchanger length.

### 3.4 Evaporator

The evaporator model is analogous to the condenser model but only two zones were considered: saturated and superheated. The fluid enters the heat exchanger in a saturated condition and may leave as superheated vapor.

### 3.5 Suction Line

The suction line was considered adiabatic in relation to the surrounding air. Therefore the refrigerant heat gain was considered equal to the heat released by the capillary tube. The pressure drop in this component was modeled using the same approach adopted in the condenser model.

### 3.6 Cabinet

An overall thermal conductance value was used to calculate the rates of heat transfer through the cabinet walls and sealing. This parameter was fitted to the experimental data generated by reverse heat flux tests.

### 3.7 Mass inventory

The volume of each component was carefully measured using the principle of a pressurized gas contained in a known volume being expanded into an evacuated and unknown volume. The system mass inventory was then evaluated from the component volumes and fluid densities. In the two-phase flow regions the void fraction concept, as described by Rice (1981), was employed to determine an average density for the working fluid. The mass of refrigerant dissolved in the lubricant was also taken into account. Several void fraction models were tested, but all of them generated a poor agreement (+20% to -70 %) with the experimental refrigerant charge. Because of this the validation study was carried out using fixed experimental values for either specific enthalpy or superheating at the evaporator outlet.

## 4. NUMERICAL PROCEDURES

The models were implemented into the commercially available software EES7 (Klein, 2004) integrated with the REFPROP7 thermodynamic and thermo-physical properties evaluation package (McLinden, 2001). The model was written in a modular format, using a specific routine for each one of the components. The main inputs and outputs of each routine were the geometric characteristics of each component, the pressure and enthalpy at the component interconnection points, the mass flow rate and the internal air temperature. Reasonable estimated values for these variables were also required as an initial condition.

Figures 4 and 5 show a comparison between predicted and measured values for the internal air temperature and compressor power consumption using the entire experimental database. As can be seen the program predictions for the internal air temperature and power consumption are within a reasonable deviation band of  $\pm 5^{\circ}\text{C}$  and  $\pm 10\%$ , respectively.

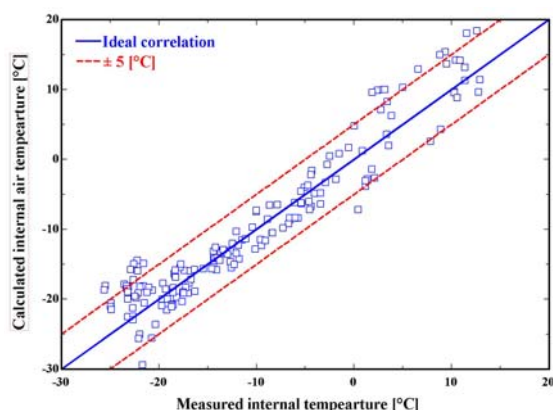


Figure 4: Internal air temperature: measured vs. predicted values

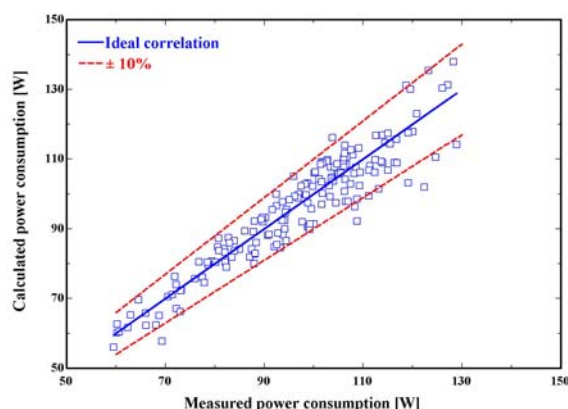


Figure 5: Power consumption: measured vs. predicted values

Figures 6 to 8 illustrate a comparison between predicted and measured values for the internal air temperature and compressor power consumption for the refrigeration system #1 (see Table 1) and for an ambient temperature of  $32^{\circ}\text{C}$ . The data are plotted as a function of the refrigerant charge, compressor speed and auxiliary expansion device

opening, respectively. A similar comparison is shown in Figure 9 for the same refrigeration system but varying the ambient temperature. In all cases the measured and predicted values are within an acceptable uncertainty band.

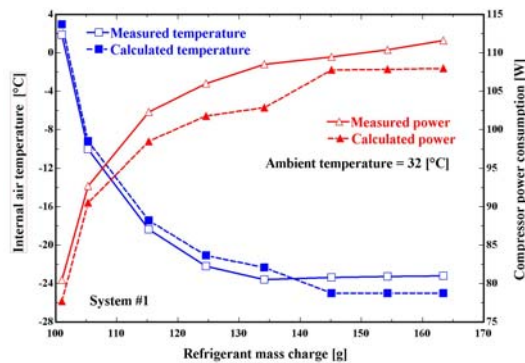


Figure 6: Measured vs. predicted values: refrigerant charge

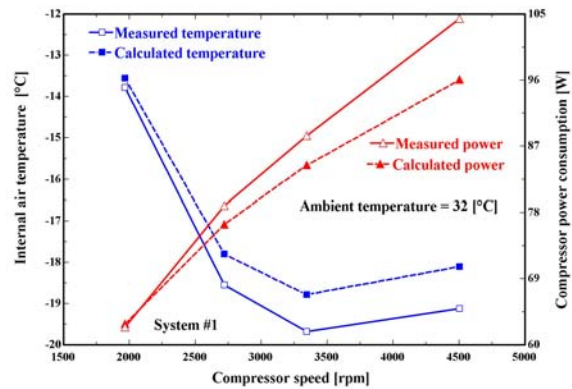


Figure 7: Measured vs. predicted values: compressor speed

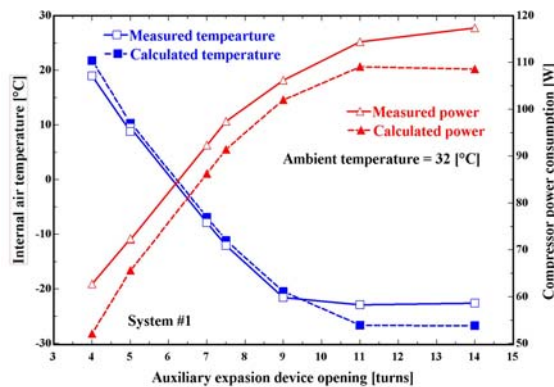


Figure 8: Measured vs. predicted values: auxiliary expansion device opening

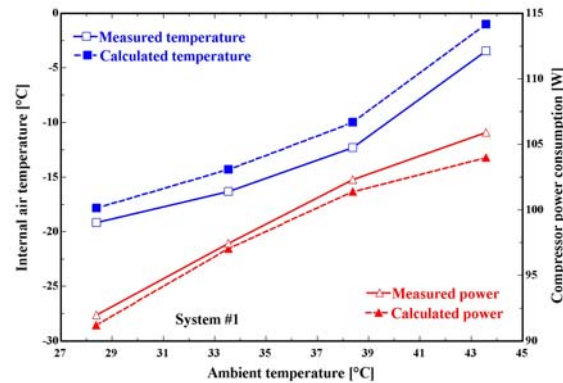


Figure 9: Measured vs. predicted values: ambient temperature

## 6. SYSTEM ANALYSIS

The validated model was here used to simulate the system #1 behavior assuming the following main conditions: (i) freezer air temperature =  $-18^{\circ}\text{C}$ , (ii) ambient temperature =  $32^{\circ}\text{C}$ , (iii) compressor speed = 4000rpm and (iv) auxiliary expansion device completely open.

The effects of the cabinet thermal conductance, capillary tube-suction line heat exchanger effectiveness, number of condenser wires and number of evaporator fins on the compressor power consumption are illustrated in Figures 10 to 13, respectively. The refrigerant charge variation needed for keeping the internal air temperature constant is also shown in these figures (dotted lines).

When the number of evaporator fins was varied (Figure 13), not only the refrigerant charge but also the compressor speed needed to be adjusted, in order to maintain the internal air temperature constant. This is a clear indication of the importance of matching the compressor and evaporator refrigerating capacities. It is also worth noting the asymptotic power consumption reduction with the augmentation of either the condenser or evaporator finned area.



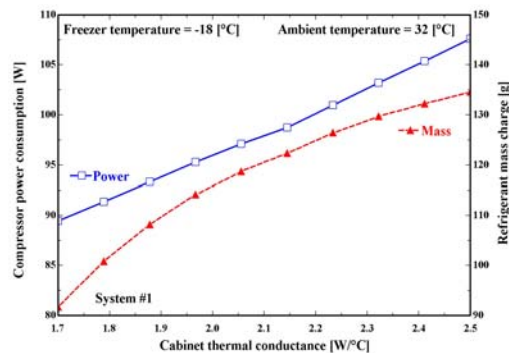


Figure 10: Effect of the cabinet thermal conductance

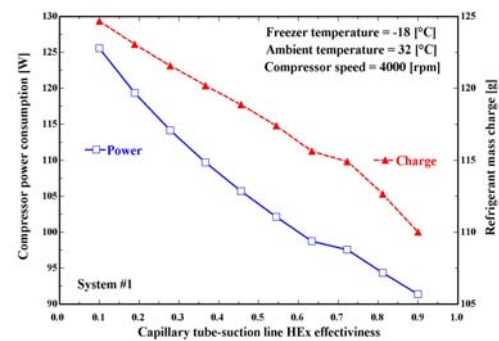


Figure 11: Effect of the Hex effectiveness

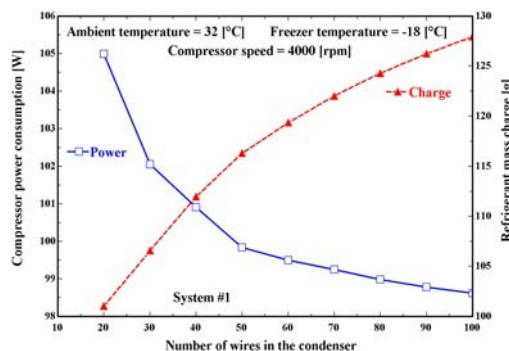


Figure 12: Effect of the condenser finned area

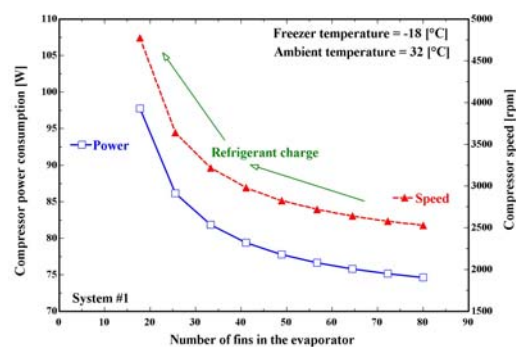


Figure 13: Effect of the evaporator finned area

Figure 14 depicts the states map for the refrigeration system#1 considering the refrigerant charge, compressor speed and the capillary tube inner diameter as state variables. This map shows a region where the compressor power reaches an optimum value. In this region both the condenser and the evaporator are fully charged, with their exits in approximately saturated conditions.

Increasing the compressor speed also increases the refrigerant charge band between an undercharged condenser and an overcharged evaporator, always with a penalty for the compressor power consumption.

This result shows an opportunity not only for the design of an almost optimum system but also for the implementation of a multi-variable control system to explore the advantages of this behavior.

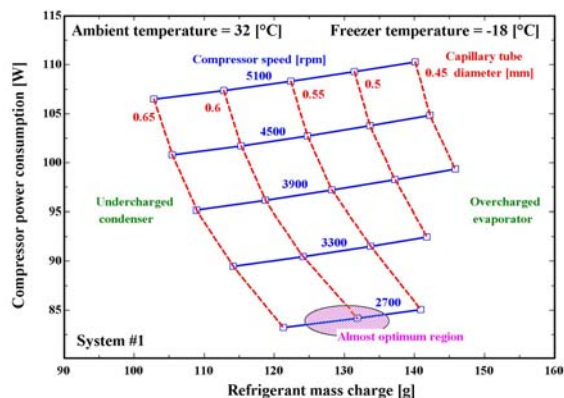


Figure 14: States map for system #1

## 7. CONCLUDING REMARKS

Conclusions of this work can be summarized as follows:

**Experiments:** A top-mount refrigerator was tested under a wide range of operating conditions. Thirteen variables were experimentally evaluated that led to over 160 data points. Refrigerant pressure and temperature measurements were taken at 7 locations along the refrigeration loop with a minimum effect on system performance. These data were essential for the development and validation of the component models.

**Models:** The mass, energy and momentum conservation equations were used as a framework for the components models. Parametric and lumped models were also developed and fitted to the experimental data. The main empirical parameters were the friction factors and the heat transfer coefficients.



**Numerical procedures:** The models were implemented into the EES/REFPROP7 software. The computer code was written in a modular format, using a specific procedure for each one of the components. When all the routines are running together the program solves a set of 12 no-linear equations. The program predictions were compared to the measured data and a reasonable level of agreement was found.

**Analysis:** The effects of some key parameters on the system performance were determined. During this analysis the internal air temperature was maintained constant reflecting a design requirement. A system states map that provides insights into both the design and control procedures was also presented.

## NOMENCLATURE

A	Area, m <sup>2</sup>	T	Temperature, K		<b>Subscripts</b>
cp	Specific heat, J/kgK	UA	Thermal conductance, W/K	amb	Ambient
D	Inner diameter, m	v	Specific volume, m <sup>3</sup> /kg	cond	Condenser
f	Friction factor	V	Refrigerant velocity, m/s	comp	Compressor
h	Specific enthalpy, J/kg	W	Compressor power, W	ext	External
htc	Heat transfer coefficient, W/m <sup>2</sup> K	ρ	Refrigerant density, kg/m <sup>3</sup>	int	Internal
L	Length, m	η <sub>s</sub>	Isentropic efficiency	liq	Liquid
m	Mass flow rate, kg/s	η <sub>v</sub>	Volumetric efficiency	sat	Saturated
N	Compressor speed, rps	ΔP	Pressure drop, Pa	sub	Sub-cooled
PD	Piston displacement, m <sup>3</sup> /s			sup	Superheated
Q	Heat transfer rate, W			vap	Vapor
R	Thermal resistance, K/W				

## REFERENCES

- ASHRAE, 2002, *Refrigeration System and Applications Handbook*, Atlanta, USA.
- Chi, J., didion, D., 1982, A Simulation Model of the Transient Performance of a Het Pump, *International Journal or Refrigeration*, 5, 176-184.
- Davis, G. L., Scott, T. C. 1976, Component Modeling Requirements for Refrigeration System Simulation, *Proc. 1976 Purdue Compressor Technology Conference*, West Lafayette, USA, 6-9 July, 401-8.
- Gosney, W. B., 1982, *Principles of Refrigeration*, Cambridge Univ. Press., Cambridge, UK.
- Kays, W. M. and London, A. L., 1984, *Compact Heat Exchanger*, Krieger Publishing, Florida, USA, 3ed., 335p.
- Kempiak, M. J. and R. R. Crawford, 1991, Three-Zone Modeling of a Mobile Air Conditioning Condenser, *ACRC Technical Report*, TR-03, April, 144 p.
- Klein, S.A., and F.L. Alvarado, 2004, *EES - Engineering Equation Solver*, Middleton, WI, F-Chart Software.
- McLinden, M. O., Klein, S. A.; Lemmon, E. W., Peskin, A. P., 2001, *NIST Thermodynamic and Transport Properties of Refrigerants and Refrigerant Mixtures – REFPROP*, Version 7.0, US-DOE, NIST, MD, USA.
- Rice, C. K., 1987, The Effect of Void Fraction Correlation and Heat Flux Assumption on Refrigerant Charge Inventory Predictions, *ASHRAE Trans.* 1987, Vol. 93(1), pp 341-367, N° 3035.
- Shah, R. K., Sekulic, D. P., 2003, *Heat Exchanger Design*, John Wiley & Sons, New Jersey, USA, 941p.
- Yasuda, H., Touber, S., Machielsen, C. H. M., 1983, Simulation Model of a Vapor Compression Refrigeration System, 1983, *ASHRAE Transactions* 1983, Vol. 89(2A):408-425.
- Zangari, J. M., 1998, *Experimental Evaluation of Concentric Capillary Tube-Suction Line Heat Exchangers Performance*, M. Sc. Thesis, Department of Mechanical Engineering, Federal University of Santa Catarina, Florianópolis, SC, Brazil (in Portuguese).

## ACKNOWLEDGMENTS

The authors are grateful to *Empresa Brasileira de Compressores* (EMBRACO S.A.) for sponsoring this research program. The continued support for this research program from *Conselho Nacional de Desenvolvimento Científico* (CNPq) is also duly acknowledged.